



Raw data and noise in spectrophotometry

Bruna Falgueras Vallbona^{a,*}, Ardiana Kajtazi^b, Golnaz Shahtahmassebi^c, Quentin S. Hanley^{d,e}

^a Department of Chemistry and Forensics, School of Science and Technology, Nottingham Trent University, Nottingham, NG11 8NS, United Kingdom

^b Separation Science Group, Department of Organic and Macromolecular Chemistry, Ghent University, Krijglaan 281, B-9000, Ghent, Belgium

^c Department of Physics and Mathematics, School of Science and Technology, Nottingham Trent University, Nottingham, NG11 8NS, United Kingdom

^d GH and Q Services Limited, West Studios, Sheffield Road, Chesterfield, S41 7LL, United Kingdom

^e College of Science and Engineering, University of Derby, Markeaton Street, Derby, DE22 3AW, United Kingdom

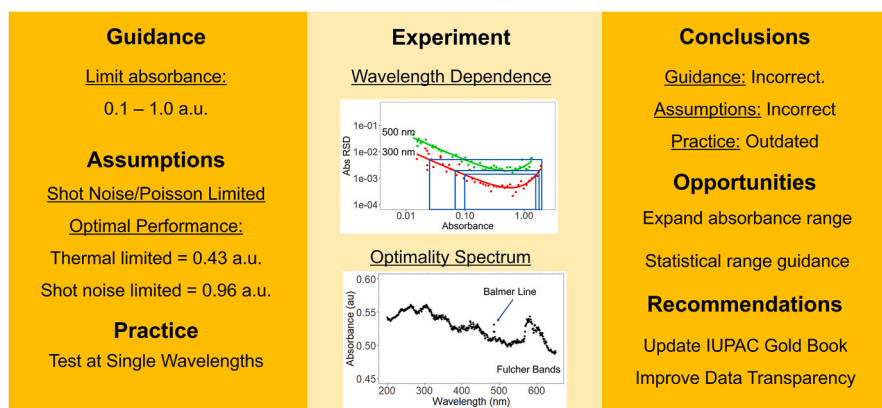
HIGHLIGHTS

- Modern spectrophotometers are not Poisson-limited.
- Optimal absorbance measurements vary with wavelength.
- To better characterize spectrophotometers, raw intensities need to be supplied by vendors.
- Manufacturers need to provide more transparency in data acquisition strategies.
- IUPAC's Gold Book references require modernisation.

GRAPHICAL ABSTRACT

Prove of wavelength dependence along the spectrum demonstrating current guidance out of date.

Raw Data and Noise in Spectrophotometry



ARTICLE INFO

Handling Editor: Xiu-Ping Yan

Keywords:

Spectrophotometer
Dispersion model
Fluctuation scaling

ABSTRACT

Background: Spectrophotometers are ubiquitous in chemical and biological science; however, their precision limits are under-appreciated. Rules-of-thumb and IUPAC referenced guidance restricting absorbance ranges to minimize uncertainty are based on historically important instruments which are no longer as widely used. Advances over the last half-century changed most “raw” data from absorbance and transmittance values directly produced in analog electronics to digitized intensities. The latter are rarely provided in favour of digitally transformed derived data. Assessment of spectrophotometer limitations using digitized intensities would be straightforward with mean-variance analysis. However, in their absence, derived data evaluated at scale allows efficient characterisation of modern spectrophotometers.

Results: This study analyses signals when I and I_0 are not available and only absorbance or transmittance are obtained. Current IUPAC referenced guidance indicates that absorbance should be limited between 0.1 and 1.0 a.u. with optimal performance (minimum relative standard deviation (RSD)) at 0.43 a.u. or 0.86 a.u. depending on

* Corresponding author.

E-mail address: N0830629@my.ntu.ac.uk (B. Falgueras Vallbona).

<https://doi.org/10.1016/j.aca.2024.343393>

Received 23 May 2024; Received in revised form 14 October 2024; Accepted 3 November 2024

Available online 5 November 2024

0003-2670/© 2024 The Authors. Published by Elsevier B.V. This is an open access article under the CC BY license (<http://creativecommons.org/licenses/by/4.0/>).

the type of limiting noise. We characterised noise in UV–Vis spectrophotometers using three methods and report optimality spectra for the first time. We found the instruments were not Poisson optimal and best RSDs were sometimes above 1.0 a.u. We could find no evidence justifying guidance restricting absorbance to between 0.1 and 1.0 a.u. Measured RSD and light intensity are more important than absorbance values for assuring good quality measurements. However, estimating light intensity is a difficult inverse problem when I and I_0 are not available, and the tested commercial instruments did not provide these.

Significance: Based on this work, classical theories are insufficient to describe spectrophotometers accurately. Furthermore, we urge IUPAC to modernise the references in its Gold Book and press instrument makers to improve data transparency. These steps are crucial to use spectrophotometers optimally.

1. Introduction

Spectrophotometry is critical in routine measurements across the chemical, physical, and biological sciences [1] where it is used to characterize and quantify molecular and biological species [2], aggregates, and materials. Spectrophotometers of varying characteristics [3–5] are found in process control, individual labs, and chromatographic systems [6]. They are robust, reliable, and comparatively inexpensive. This led to a range of methods for characterizing the instruments and specifying standards and there is in-depth theory describing their behaviour [7,8]. The importance of spectrophotometry has resulted in regular reviews of the subject and available instrumentation [6,9]. Although theories of limiting uncertainty have been available for some time [8,10], verification in modern instruments has tended to treat individual instruments and wavelengths in isolation [3,8,9].

A range of mathematical descriptions are available for the relationship between absorbance and the relative standard deviation (RSD) in a spectrophotometer. These consider thermal noise, photon noise, cuvette resetting variability, source fluctuation, and general photometric error. The most relevant ones predict minima in the range from 0.43 to over 1.0 absorbance units (a.u.). Most include an assumption that the light source is Poisson (shot noise) unless it is subject to “flicker”. Much of the classic work was done with few measurements by modern standards due to limitations of the time [10]; however, the conclusions obtained still inform current practice. For example, IUPAC’s Gold book [11] currently refers to a 1988 document with recommendations indicating a necessity to keep absorbances between 0.1 and 1 a.u. and best results will be obtained at 0.43 a.u. for “thermal” noise or 0.86 a.u. for “shot noise” [1]. This guidance needs review. The 0.43 a.u. value is for mostly archaic instruments having linear transmittance readouts with constant variance [12,13]. It is unclear the source for the 0.86 a.u. value (possibly a misprint) as it has long been known from both theory and practice that 0.96 a.u. is the correct value for variance proportional to signal [8,14]. In modern instruments, it is possible to get excellent results outside the 0.1 to 1.0 a.u. range and, poor results can be obtained at any absorbance including near 0.43 a.u., 0.96 a.u., or any measured optimum values.

The last half century has seen a fundamental advance in spectrophotometer design. The most profound of these is the shift from transmittance and absorbance data produced by dedicated electronics to these quantities being generated in software using digitized intensity values. The consequence of this is profound. In the former, transmittance and absorbance values are the primary data. In the latter, the primary data are digitized intensity values representing I and I_0 . Further, both I and I_0 are implicit in many formulas for precision in absorbance and transmittance measurements [10,15] with noise in the intensities limited by Poisson or other distributions. To assess agreement with theory, these primary data (values representing I and I_0) are essential. However, commercial instruments do not usually provide this primary data and recovering estimates of the primary data is a difficult inverse problem. For single absorbance measurements, recovery is impossible.

To investigate current IUPAC referenced guidance and understand the behaviour of modern instruments, we investigated reproducibility in four UV–Vis spectrophotometers under a range of conditions. We also

investigated ways to recover I and I_0 , found optimal absorbance values, and assessed the extent to which they matched the best case for a Poisson limited system.

2. Theory

The amount of light fundamentally limits the precision of spectrophotometric measurements. Theoretical precision improves with increased light intensity due to the statistical properties of light. Here, measured precision represents replicate measurements made on samples without replacing the sample or cuvette. When the light source is not number squeezed [16,17], the Poisson distribution defines the best-case limits on fluctuations in a coherent light source with a given number of photons (often referred to as shot noise) [8,18,19]. The Poisson distribution is a special case of power variance (equation (1)) where $\alpha = 1$ [20,21].

$$\sigma^2 = \mu^\alpha \quad (1)$$

In this presentation, variance, σ^2 , is related to the mean value, μ , via an exponent, α . Empirically, a system with power variance can be assessed by log-log plots of variance (\bar{x}, s^2) or standard deviation (\bar{x}, s), where s is the sample standard deviation. For Poisson distributed light intensities, the slopes would be 1.0 and 0.5 for variance and standard deviation, respectively [21]. Earlier work has also investigated source flicker as variance proportional to signal squared ($\alpha = 2$) [8]. Although Poisson behaviour limits the precision of transmittance and absorbance measurements, proving a particular instrument achieves this limit is difficult in the absence of the raw intensity values. If the raw intensity values are available, the variance can be assessed directly via the method of mean variance [22,23]. If only derived values (e.g., absorbance and transmittance) are provided, the same assessment is non-trivial. In the absence of raw intensity values, we tried three ways of assessing whether the spectrophotometers were achieving Poisson behaviour: transmittance fluctuations in the absence of sample, light source additivity, and minimum relative standard deviation (RSD).

Method of Transmittance = 1: The simplest approach to model uncertainty in spectrophotometry is to assume it consists only of a light source with intensity, I_0 , which is attenuated by a sample to a new intensity, I . Transmittance, T , is the ratio of I over I_0 , and applying error propagation rules the uncertainty in transmittance and absorbance are [24].

$$s_T = T \sqrt{\left(\frac{s_I}{I}\right)^2 + \left(\frac{s_{I_0}}{I_0}\right)^2} \quad \text{and} \quad s_A = 0.4343 \sqrt{\left(\frac{s_I}{I}\right)^2 + \left(\frac{s_{I_0}}{I_0}\right)^2} \quad (2)$$

If the light source is Poisson and $T = 1$, then $I = I_0$ and $s_{I_0} = s_I = \sqrt{I_0}$. Substituting into equation (2) and rearranging yields an estimate for light intensity in photon units that can be evaluated with a series of replicate transmittance measurements.

$$I_{est,0} = \frac{2}{s_T^2} \quad (3)$$

This only represents intensity when the system has power variance with $\alpha = 1$ as expected for a Poisson system. If read noise or stray light is

Poisson in nature, these can be estimated by blocking the light path at the cuvette. When the system has power variance with $\alpha \neq 1$, equation (3) provides an intensity-related metric but will incorrectly estimate photon numbers.

Method of Source Additivity: In instruments with deuterium (D) and tungsten (W) light sources, the total intensity as determined by equation (3) must equal the sum of the intensities determined using the same method for the lamps singly.

$$I_{0, \text{total}, s_T} = I_{0, D, s_T} + I_{0, W, s_T} \quad (4)$$

This indicates that intensities estimated from the variance of transmittance (equation (3)) for both lamps together will be the sum of the D and W intensities measured individually. Equation (4) only holds for power variance with $\alpha = 1$. Where the equality (equation (4)) does not hold, this falsifies the assumption of a Poisson-limited measurement of the light source.

Method of Minimum RSD: Conformity with a Poisson source can be assessed by measuring a set of samples over a wide range of concentrations to find the absorbance of minimum RSD. Existing theory indicates the minimum for a Poisson noise limited system should be 0.96 a.u. [14]. In a hybrid system of Poisson and charge coupled device (CCD) or diode array (DA) amplifier read noise, the position of the minimum will decrease depending on the relative contributions of light and amplifier noise. The hybrid system can be modelled by $s_{I_0} = \sqrt{I_0}$, $s_T = \sqrt{I} = \sqrt{T * I_0}$ considering transmittance the ratio of I over I_0 , and by introducing read noise to equation (2).

$$s_T = T \sqrt{\frac{T * I_0 + m^2}{(T * I_0)^2} + \frac{I_0 + m^2}{I_0^2}} \text{ and } s_A = 0.4343 \sqrt{\frac{T * I_0 + m^2}{(T * I_0)^2} + \frac{I_0 + m^2}{I_0^2}} \quad (5)$$

If read noise is constant at all wavelengths, equation (5) predicts the minimum position, and hence the optimal absorbance for making measurements will vary with wavelength due to source(s) intensity variation. The minima can be found empirically at each wavelength and plotted as an optimal performance spectrum. The values of the minima can then be compared to expectations from prior work and IUPAC referenced guidance [1].

3. Experimental section

Measurements were made using two single-beam UV-Vis diode array spectrophotometers (Agilent Technologies Cary 8454), a double beam diode array UV-Vis spectrophotometer (PerkinElmer Lambda 25 UV/VIS Spectrometer) and a single beam multi-cuvette UV-Vis spectrophotometer (UV5Bio Mettler Toledo).

The two Cary 8454s (Cary 1 and Cary 2) and the Lambda 25 covered from 190 to 1100 nm at 1 nm intervals and the UV5Bio from 190 to 1100 nm at 0.2 nm intervals. The spectrophotometers were tested using 3 types of experiments taking replicate spectra ($n = 10$) for each of a set of conditions: i) replicate measurements in the absence of samples or cuvettes (Method of $T = 1$); ii) similar measurements made while switching on and off the deuterium and the tungsten lamps (Method of Source Additivity); iii) measurements of 48 dye containing solutions of varying absorbance (Method of Minimum RSD). Measurements were made without resetting cuvettes for the 10 replicates for the two Cary and the Lambda 25. The UV5Bio had an automated reset movement. The UV5Bio had single light source (Xe flashlamp) and the Lambda 25 does not combine its two light sources making them unsuitable for source additivity tests. The dye set did not yield a minimum at many wavelengths in the UV5Bio.

For the minimum RSD measurements, 48 solutions were prepared from a stock solution containing E102, E124, E133 and E155 (APC Pure; Hyde, Cheshire, UK) nominally 16.5 ppm of each. This mixture was engineered to have absorbances from near 0 to over 1.0 a.u. in the range 200–650 nm toward a goal of finding RSD minima between 0.43 and

0.96 a.u. Results were obtained in absorbance units and the standard deviation ($n = 10$) divided by the mean was used to obtain RSD values. Minima were found and reported in two ways: i) non-linear least squares fits to equation (5) using R/RStudio (from 200 to 650 nm, except for Cary 1 where equation (5) did not converge between 200 and 300 nm), or ii) the lowest value in the absence of a minimum (UV5Bio between 200 and 650 nm). The minima were plotted as optimal absorbance spectra.

The $T = 1$ and source additivity data were analysed using R (version 4.2.2) [25] and RStudio (2022.07.1 build 554) [26] which were also used to organise, plot and analyse the minimum RSD data using ggplot2 (3.4.0) [27], ggpubr (0.4.0) [28], matrixStats (0.62.0) [29], and nlstools (2.0-0) [30] packages. Fitting of equation (5) was done in R with *nlstools()* with initial values of $I_0 = 10^7$ and $m = 1200$ and assuming constant m for all pixels [19]. The *optimise()* function from R identified the RSD minima for each individual wavelength for both Cary 8454s and the Lambda 25, and all instruments' results were plotted with ggplot2.

4. Results and discussion

4.1. Statistical source intensity estimates

Statistical intensity estimates were obtained by replicate ($n = 10$) measurements of transmission spectra in the absence of sample or cuvettes. From the standard deviations and equation (3), the statistical intensity spectrum ($I_{\text{est},0}(\lambda)$) of the light source was assessed (Fig. 1). The recovered spectra from the two Cary 8454s revealed (Fig. 1a and b) the H_γ , H_β and H_α Balmer lines of deuterium at 434, 486, and 656 nm respectively [31,32]. There were also signs of the Fulcher bands and other features seen in published spectra of deuterium lamps [33]. It is important to note that the lamp intensity varied with wavelength by up to 5 orders of magnitude. Given this variation, it is unclear that all wavelengths are being collected equivalently when absorbance measurements are made. For example, a photodiode array with a well capacity of 300 ke⁻ would have some pixels close to saturation while others might be only collecting 30 e⁻. Without careful data collection strategies, the pixels with only 30 e⁻ will give poor measurements. The intensity was highest in the UV and lowest above 900 nm.

The corresponding experiment with the Lambda 25 was conducted, and the Balmer and Fulcher bands were absent (Fig. 1c). However, this instrument does not direct both lamp beams through the optical system simultaneously. The halogen lamp is blocked during measurements in the UV range, while the deuterium lamp is blocked in the visible range [34]. Consequently, Balmer and Fulcher bands are not observed, as they occur above 434 nm, where deuterium radiation is blocked by the instrument. There is, however, a region in the spectrum between 327 and 385 nm where light intensity drops by 2 orders of magnitude as the lamps are switched. Similar experiments with the UV5Bio resulted in spectra with few identifiable features (Fig. 1d). This instrument employs a Xe flashlamp and showed a flat and relatively featureless spectrum with an apparent increase of intensity above 900 nm [35]. Below 900 nm, intensity varied within 2 and 3 orders of magnitude and there were no observable features corresponding to those expected from Xe lamps using this experiment. The method was readily interpretable in both Cary 8454s but not in the Lambda 25 and UV5Bio. We ascribe this to both Cary 8454s achieving closer to Poisson limitation under these conditions than the Lambda 25 and the UV5Bio.

4.2. Method of Source Additivity

Statistical determinations of $I_{\text{est},0}$ represent photon intensity when the light source exhibits Poisson-limited behaviour. To assess the extent to which the light sources corresponded to this ideal condition, $I_{\text{est},0}(\lambda)$ was measured under four conditions (Fig. 2a): i) the combined light sources, ii) the deuterium light source, iii) the tungsten light source; and iv) with the beam physically blocked (to estimate residual stray light and

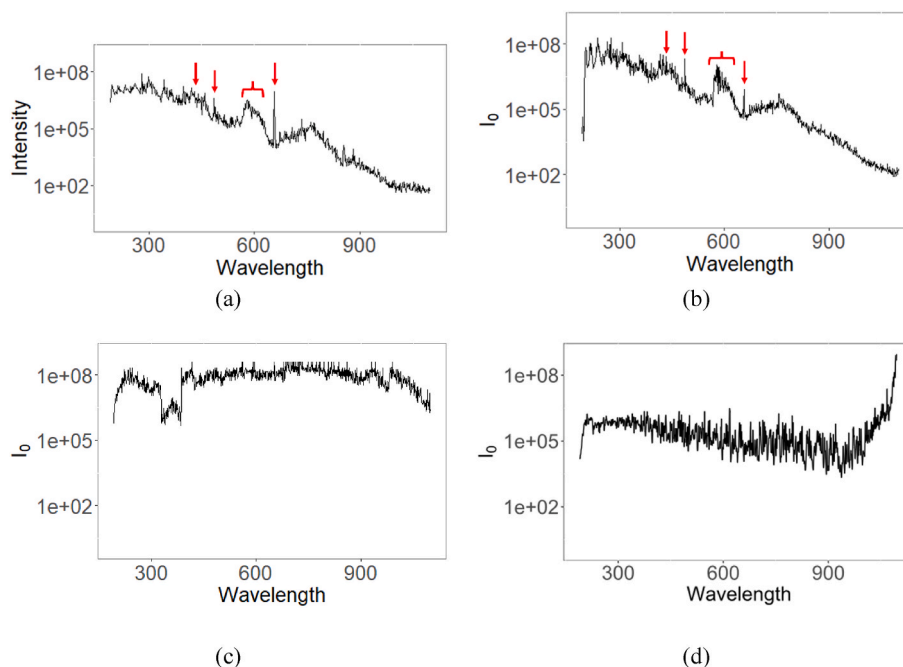


Fig. 1. Intensity spectra estimated using equation (3). (a) Cary 1 and (b) Cary 2 with log y-axis over the wavelength range from 190 to 1100 nm versus I_0 . H_γ , H_β and H_α Balmer lines of the deuterium lamps are noted with red arrows at 434, 486 and 656 nm, respectively, and Fulcher bands noted with a red brace. (c) Lambda 25 with log y-axis over the range from 190 to 1100 nm at 1 nm intervals. (d) UV5Bio with log y-axis over the range from 190 to 1100 nm at 0.2 nm intervals. (For interpretation of the references to colour in this figure legend, the reader is referred to the Web version of this article.)

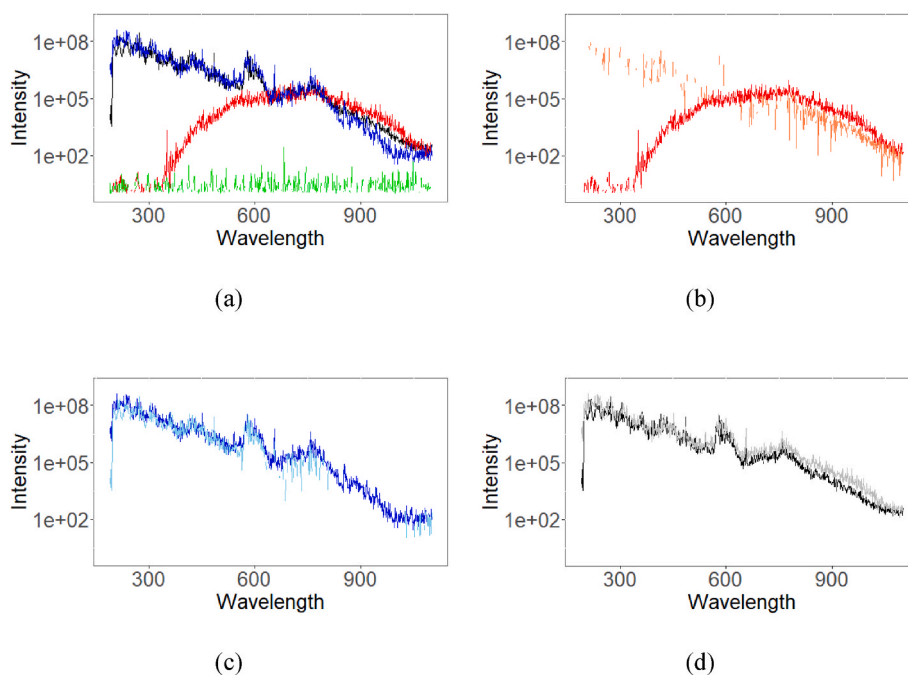


Fig. 2. Plots of the estimated intensities for the light sources in isolation, combined, and by difference on a logarithmic scale for both Cary 2. (a) Direct estimates for both lamps (black), deuterium lamp (blue), tungsten lamp (red), and blocked beam (green). (b) Tungsten lamp intensity estimated directly (red) and by difference (orange). (c) Deuterium lamp intensity estimated directly (blue) and by difference (light blue). (d) Combined intensity of both lamps estimated directly (black) and by summing the tungsten and deuterium lamp intensities (grey).

Note: These logarithmic plots omit regions where the differences are negative. In panel (b), this occurs below approximately 650 nm and in panel (c) between approximately 775 and 1060 nm. (For interpretation of the references to colour in this figure legend, the reader is referred to the Web version of this article.)

dark signal). The laboratory conditions were 20.5 °C with 58 % humidity and 20.8 °C with 45 % humidity for Cary 1 and 2, respectively. This method gives the light source the best opportunity to dominate relative to other noise sources because there is no attenuation of the

beam when $T = 1$. This method was only possible in the Cary 8454 instruments since the Lambda 25 lamps do not coexist at any wavelength and the UV5Bio had only a single light source. Cary 2 is discussed and plotted below (Fig. 2) and Cary 1 is presented in the supplementary

material (Fig. S1). Both instruments exhibited similar behaviour.

With the beam blocked (Fig. 2, panel (a), green), the estimated dark signal was 2.87 ($n = 796$) with 115 undefined values returned for wavelengths ($s_T = 0$). This level of dark noise is likely unrealistically low for a photodiode array suggesting some combination of offset subtraction and trapping of high and low absorbance values. Using the recovered values of $I_{est,0}(\lambda)$, the tungsten light source (Fig. 2, panel (a), red)

was estimated to be brighter alone than the combined intensity of both lamps estimated together (Fig. 2, panel (a), black) above 640 nm. When the tungsten lamp was estimated by difference (Fig. 2, panel (b), orange) as $I_{0,W,s_T} = I_{0,total,s_T} - I_{0,D,s_T}$ and compared to the result obtained in isolation (Fig. 2, panel (b), red) The spectrum measured by difference (orange) was consistently low above 800 nm. Below 800 nm, many negative values were obtained which do not appear on the log-scale

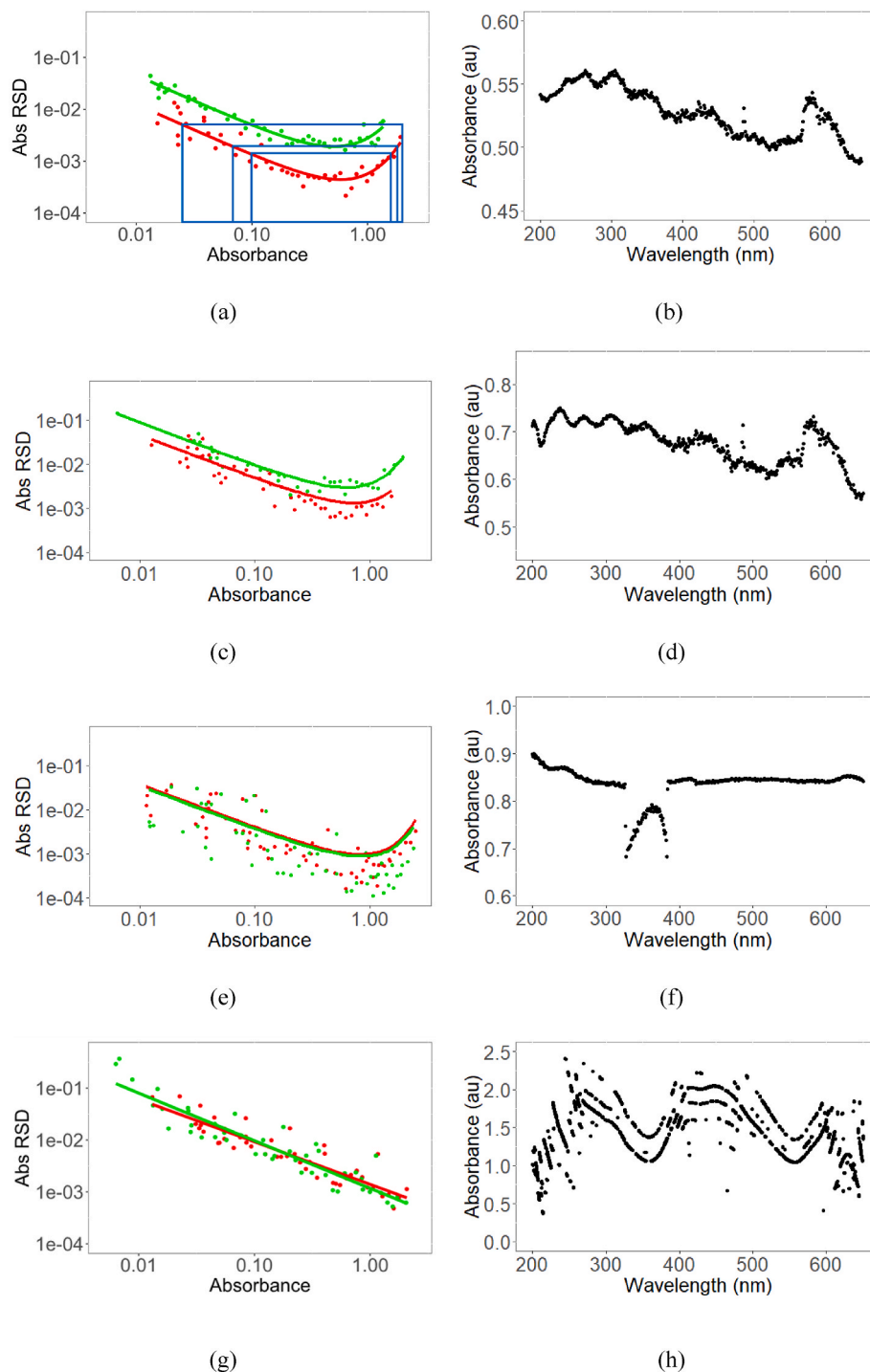


Fig. 3. (a) Cary 1 logarithmic plot of absorbance versus its relative standard deviation (RSD) for the non-linear fitting functions of equation (5) for 300 nm (red) and 500 nm (green). Blue boxes illustrate inconsistencies in standard measurement guidelines (see text for details). (c), (e) and (g) logarithmic plots of absorbance versus RSD for the linear fit of the logarithmic scale of the data for 300 nm (red) and 500 nm (green) for Cary 2, Lambda 25 and UV5Bio, respectively. (b), (d) and (f) Positions of the minima from fits to equation (5) for Cary 1, Cary 2, and Lambda 25 over 200–687 nm, 190–817 nm, and 190–1100 nm, respectively. (h) UV5Bio positions of the minima from the absorbance location of the minimum RSD obtained for each wavelength from 190 to 700 nm. (For interpretation of the references to colour in this figure legend, the reader is referred to the Web version of this article.)

graph. The deuterium intensity in isolation (Fig. 2, panel (c), blue) was similar to that obtained by difference (Fig. 2, panel (c), light blue) across the UV and much of the visible; however, above 750 nm, negative values were obtained. This would occur if the deuterium lamp had excess noise which leads to lower estimates of lamp intensity by equation (2). Finally, when calculated as the sum of the deuterium and tungsten intensity estimates (Fig. 2, panel (d), grey) exceeded the measured (Fig. 2, panel (d), black). In summary, the spectra estimated in isolation could not be obtained by sum or difference for either of the two instruments. This indicates the light sources were not achieving the often-assumed Poisson-limited behaviour. In both instruments, the Balmer lines and Fulcher bands only appeared if the deuterium lamp was on and were not seen in the blocked beam and tungsten lamp experiments. This argues for the value of the method for providing an intensity related metric, even when ideal Poisson behaviour is not observed.

4.3. Method of Minimum RSD

The previous methods assessed the spectrophotometers under conditions of no attenuation ($T = 1$; $Abs = 0$). Assessing the position of the minimum and the shape of the RSD curve (equation (5)) with a set of dye solutions provides information about behaviour under more realistic conditions. Using these, a set of (Abs , RSD) plots were generated over the wavelength ranges of the instruments. Example RSD curves at 300 and 500 nm illustrate differences between both Cary 8454s (Fig. 3a and c), Lambda 25 (Fig. 3e) and UV5Bio (Fig. 3g) as well as limitations of IUPAC referenced guidance. For both Cary 8454s, the RSD curves at 300 nm (Fig. 3a and c) are lower than at 500 nm and the position of the minimum shifted to higher absorbance due to greater light intensity at 300 nm. The Lambda 25 plot (Fig. 3e) shows overlap between the two wavelengths. The $nls()$ fits to the Lambda 25 data did not align well with the experimental data giving modelled RSDs consistently higher than the experimental results. However, the positions of the minima gave a consistent trend. The 300 nm and 500 nm RSD plots for UV5Bio (Fig. 3g) were linear, the responses overlapped, and neither wavelength reached an obvious minimum.

When the RSD minima are plotted as a spectrum, both Cary 8454s (Fig. 3b and d) revealed features consistent with the spectrum of the illumination sources (e.g.: as in Fig. 1, the H_β and H_γ Balmer lines and Fulcher bands are present). Similarly, the Lambda 25 (Fig. 3f) exhibited a drop in the absorbance minima at the lamp switch consistent with the source intensity characteristics in Fig. 1, panel (c). Conversely, the UV5Bio RSD minima spectrum (Fig. 3h) had features consistent with the spectrum of the dye set. The UV5Bio also exhibited what appear to be parallel spectra spaced approximately 0.1–0.3 a.u. apart. We ascribe this to adaptive measurement increasing the number of scans during acquisition. These contrasting features provide a framework for using RSD behaviour to assess IUPAC referenced and other related guidance [1].

The IUPAC referenced and related guidance indicates absorbance measurements need to be taken between 0.1 a.u. and 1 a.u. It further suggests the minimum RSD should be at 0.43 a.u. or 0.96 a.u. (correcting for possible misprint) depending on the limitations imposed by the type of spectrophotometer. Consideration of Fig. 3 indicates this needs revision. i) If the RSD observed at 0.1 a.u. is the limit of what is acceptable and the 300 nm curve is the reference, then no part of the 500 nm curve is acceptable (Fig. 3a, inner box). ii) The minimum uncertainty at 500 nm justifies a range of absorbance values at 300 nm that extend well beyond the 0.1 to 1.0 a.u. range in IUPAC referenced guidance (Fig. 3a, middle box). iii) If the uncertainty associated with the 500 nm curve at 0.1 a.u. is acceptable, that defines a region on the 300 nm RSD curve extending from less than 0.03 to over 2.0 a.u. (Fig. 3a, outer box). iv) Neither Cary 8454 (1 or 2) nor Lambda 25 returned an RSD minimum matching either 0.43 or 0.96 a.u. v) The guidance in the IUPAC referenced document is completely inappropriate for the UV5Bio. The best RSD is found well above 1.0 a.u. at nearly every wavelength. The

exceptions are due to the dye set and a few possibly spurious values (possibly due to adaptive acquisition). These results indicate current guidance based on arbitrary absorbance values and mostly archaic spectrophotometers should be discarded and replaced with guidance on acceptable RSD or better documentation of light intensity and its noise characteristics.

In addition to being a challenge to current guidance, these observations indicate that RSD behaviour measured at a single wavelength should be used with caution. Most prior work has implicitly assumed that acceptance obtained at one wavelength generalizes across the spectrum. Fig. 3b, d, 3f and 3h make clear that measured RSD can change dramatically in the space of a few nm (e.g., in the region of the H_β Balmer line (Cary 8454s), a lamp switch (Lambda 25) or nearly everywhere (UV5Bio)). Variations in light intensity and other noise sources require better access to the raw intensity measurements than the current generation of commercial instruments provide. Data preservation and access in modern instruments appears to be designed based on archaic spectrophotometers.

To set guidance or acceptance criteria for spectrophotometers, the noise from light source fluctuations and other noise needs to be assessed; however, in the absence of raw intensity data, this is difficult. Equations (3) and (5) allow intensity to be estimated for Poisson light sources, but none of the instruments behaved in a Poisson limited way. Even with a Poisson system, the inverse problem of recovering I_0 and I would be difficult using a set of carefully designed absorbing solutions as done here. In the case of individual absorbance or transmittance measurements, recovery of the raw data (individual I_0 and I values) is simply impossible *unless instrument manufacturers provide them*.

5. Conclusions

This study demonstrates these spectrophotometers were not Poisson-limited. This includes best-case measurements ($T = 1$, $Abs = 0$; Fig. 1) and conditions of typical use (Fig. 3). Based on the data collected, standard guidance for making best measurements (e.g., absorbance between 0.1 and 1.0 a.u.) does not arise from any theory or defensible statistical reasoning. This guidance, versions of which have been widely taught for many years [36–38], is completely inappropriate for modern instruments. The absorbance limits indicated in the guidance are arbitrary, too restrictive and expectations of optimal conditions for measurement do not match the behaviour of the modern instruments we tested. It is better to define an acceptable RSD and verify this with replicate measurements than assume some arbitrary absorbance range will provide this. Although there may be chemical reasons to limit the range of absorbance, high quality spectrophotometric measurements can be made outside these arbitrary limits. It is also important to verify this at the wavelength(s) of interest. The intensity of light varies across the spectrum such that tests done at a single wavelength do not generalise to the whole spectrum or even wavelengths close by.

Most importantly, the guidance IUPAC refers to in its Gold Book and data reporting by instrument manufacturers need to be modernised. The guidance is archaic and misleading. Manufacturers need to give access to spectrophotometric raw data and be more transparent about data acquisition strategies. These are essential for better quality assurance and raise important issues related to compliance with regulatory requirements and data preservation.

CRedit authorship contribution statement

Bruna Falgueras Vallbona: Writing – original draft, Visualization, Software, Formal analysis, Data curation. **Ardiana Kajtazi:** Methodology, Conceptualization. **Golnaz Shahtahmasebi:** Supervision, Software. **Quentin S. Hanley:** Writing – review & editing, Supervision, Conceptualization.

Declaration of competing interest

The authors declare that they have no known competing financial interests or personal relationships that could have appeared to influence the work reported in this paper.

Acknowledgements

We would like to express our gratitude to Dr Sam Kilgour and Dr Stephen Davies for granting access to the PerkinElmer instrument at University of Nottingham and to Dr David Kilgour for his helpful discussions that guided the article to completion.

Appendix A. Supplementary data

Supplementary data to this article can be found online at <https://doi.org/10.1016/j.aca.2024.343393>.

Data availability

Data will be made available on request.

References

- [1] K. Laqua, W.H. Melhuish, M. Zander, *Molecular absorption spectroscopy, ultraviolet and visible (UV/VIS)*, *Pure Appl. Chem.* 60 (9) (1988) 1449–1460.
- [2] D. Ramos-Gonzalez, A. Davison, Qualitative and quantitative methods show stability in patterns of *cepaea nemoralis* shell polymorphism in the pyrenees over five decades, *Ecol. Evol.* 11 (11) (2021) 6167–6183, <https://doi.org/10.1002/ECE3.7443/FORMAT/PDF>.
- [3] Z. Xu, D.W. Larsen, Development of ultra-low-noise spectrophotometry for analytical applications, *Anal. Chem.* 77 (2005) 6463–6468, <https://doi.org/10.1021/ac0510134>.
- [4] P.R. Desjardins, D.S. Conklin, NanoDrop microvolume quantitation of nucleic acids, *JoVE* 45 (2010) e2565, <https://doi.org/10.1002/0471142727.mba03js93>.
- [5] Z. Bajuszova, Z. Ali, S. Scott, L.N. Seetohul, M. Islam, Cavity-enhanced immunoassay measurements in microtiter plates using BBCEAS, *Anal. Chem.* 88 (10) (2016) 5264–5270, <https://doi.org/10.1021/acs.analchem.6b00375>.
- [6] L.C. Passos M, M.F.S. Saraiva, M.L. Detection, UV-visible spectrophotometry: detectors, detection systems, and detection strategies, *Measurement: J. Int. Meas. Confed.* 1 (2019) 896–904, <https://doi.org/10.1016/j.measurement.2018.12.045>, Elsevier B.V. March.
- [7] R.W. Burke, E.R. Deardorff, O. Menis, Liquid absorbance standards, *J Res Nat Bur Stand Sect A Phys Chem* 76 A (5) (1972) 469–482, <https://doi.org/10.6028/jres.076A.041>.
- [8] L.D. Rothman, S.R. Crouch, Jr J.D. Ingle, Theoretical and experimental investigation of factors affecting precision in molecular absorption spectrophotometry, *Anal. Chem.* 47 (8) (1975) 1226–1233.
- [9] J. Galbán, S. De Marcos, I. Sanz, C. Ubide, J. Zuriarrain, Uncertainty in modern spectrophotometers, *Anal. Chem.* 79 (13) (2007) 4763–4767, <https://doi.org/10.1021/ac071933h>.
- [10] K.L. Ratzlaff, D.F.S. Natusch, Theoretical assessment of precision in dual wavelength spectrophotometric measurement, *Anal. Chem.* 49 (14) (1977) 2170–2176, <https://doi.org/10.1021/ac50022a018>.
- [11] Absorbance Matching, in: *The IUPAC Compendium of Chemical Terminology*, International Union of Pure and Applied Chemistry (IUPAC), Research Triangle Park, 2006, <https://doi.org/10.1351/goldbook.A00029>. NC.
- [12] N.T. Griggeman, Reliability of photoelectric photometry, *Anal. Chem.* 24 (3) (1952) 445–449.
- [13] F. Twyman, G.F. Lothian, Conditions for securing accuracy in spectrophotometry, *Proc. Phys. Soc.* 45 (1933) 643–662.
- [14] H.V. Malmstadt, M.L. Franklin, G. Horlick, Photon counting for spectrophotometry, *Anal. Chem.* 44 (8) (1972) 63–76.
- [15] Q.S. Hanley, C.W. Earle, F.M. Pennebaker, S.P. Madden, M. Bonner Denton, Charge-transfer devices in analytical instrumentation, *Anal. Chem. News Featur.* (1996) 661–667.
- [16] H. Vahlbruch, M. Mehmet, S. Chelkowski, B. Hage, A. Franzen, N. Lastzka, S. Gößler, K. Danzmann, R. Schnabel, Observation of squeezed light with 10-DB quantum-noise reduction, *Phys. Rev. Lett.* 100 (3) (2008) 1–4, <https://doi.org/10.1103/PhysRevLett.100.033602>.
- [17] H. Vahlbruch, M. Mehmet, K. Danzmann, R. Schnabel, Detection of 15 DB squeezed states of light and their application for the absolute calibration of photoelectric quantum efficiency, *Phys. Rev. Lett.* 117 (110801) (2016) 1–5, <https://doi.org/10.1103/PhysRevLett.117.110801>.
- [18] J. Ingle, S. Crouch, Signal-to-Noise expressions for absorption measurements, in: *Spectrochemical Analysis*, Prentice Hall, New Jersey, 1988, pp. 150–154.
- [19] G.W. Ewing, Signal to noise optimization in chemistry - Part One, *Chem. Instrum.* 45 (7) (1968) 533–544.
- [20] B. Jørgensen, Exponential dispersion models, *J. Roy. Stat. Soc. B* 49 (2) (1987) 127–145, <https://doi.org/10.1111/j.2517-6161.1987.tb01685.x>.
- [21] W.S. Kendal, A stochastic model for the self-similar heterogeneity of regional organ blood flow, *Proc. Natl. Acad. Sci. U.S.A.* 98 (3) (2001) 837–841.
- [22] R.P. Sperline, A.K. Knight, C.A. Gresham, D.W. Koppenaal, G.M. Hieftje, M. B. Denton, Read-noise characterization of focal plane array detectors via mean-variance analysis, *Appl. Spectrosc.* 59 (11) (2005) 1315–1323.
- [23] L. Mortara, A. Fowler, Evaluations of charge-coupled device (CCD) performance for astronomical use, *Solid State Imagers for Astron.* 290 (1981) 28–33.
- [24] Q.S. Hanley, Chemical measurement and fluctuation scaling, *Anal. Chem.* 88 (24) (2016) 12036–12042, <https://doi.org/10.1021/acs.analchem.6b02335>.
- [25] R Core Team, R: A Language and Environment for Statistical Computing, R Foundation for Statistical Computing, Vienna, Austria, 2022. <https://www.R-project.org/>.
- [26] RStudio Team, RStudio: Integrated Development Environment for R. RStudio, PBC, Boston, MA, 2022. <http://www.rstudio.com/>.
- [27] H. Wickham, *Ggplot2: Elegant Graphics for Data Analysis*, Springer-Verlag, New York, 2016. <https://ggplot2.tidyverse.org>.
- [28] A. Kassambara, Ggpubr: “ggplot2” based publication ready plots. <https://CRAN.R-project.org/package=ggpubr>, 2020.
- [29] H. Bengtsson, MatrixStats: functions that apply to rows and columns of matrices (and to vectors). <https://CRAN.R-project.org/package=matrixStats>, 2021.
- [30] F. Baty, C. Ritz, S. Charles, M. Brutsche, J.-P. Flandrois, M.-L. Delignette-Muller, A toolbox for nonlinear regression in {R}: the package {nlstools}, *J. Stat. Software* 66 (5) (2015) 1–21, <https://doi.org/10.18637/jss.v066.i05>.
- [31] G.A. Khayrallah, Electron impact dissociation of molecular hydrogen and deuterium: production of atomic hydrogen and deuterium α , β , and γ balmer lines, *Phys. Rev.* 13 (6) (1976) 1989–2003.
- [32] A.D. Ash, T.T.C. Jones, E. Surrey, D. Ćirić, S.I. Hall, D. Young, M. Afzal, L. Hackett, I.E. Day, R. King, JET neutral beam duct optical interlock, *Fusion Eng. Des.* 96–97 (2015) 396–399, <https://doi.org/10.1016/j.fusengdes.2015.03.010>.
- [33] G.S. Fulcher, Spectra of low potential discharges in air and hydrogen, *Astrophys. J.* 37 (1913) 60–71, <https://doi.org/10.1086/141978>.
- [34] *Lambda 25, 35, 45 User’s Guide*, Artisan Technology Group: Beaconsfield, 2000, pp. 1–116. www.artisanng.com.
- [35] J.H. Goncz, P.B. Newell, Spectra of pulsed and continuous xenon discharges, *J. Opt. Soc. Am.* 56 (1) (1966) 87–92.
- [36] H.A. Strobel, W.R. Heineman, *Chemical Instrumentation: A Systematic Approach*, third ed., Wiley, New York, 1989.
- [37] D.A. Skoog, F.J. Holler, T.A. Nieman, *Principles of Instrumental Analysis*, fifth ed., Saunders, Philadelphia, 1998.
- [38] D.C. Harris, Fundamentals of spectrophotometry, in: J. Fiorillo (Ed.), *Quantitative Chemical Analysis*, Bleyer, Craig, New York, 2007, pp. 378–401.